Coupling of simultaneously acquired electrophysiological and haemodynamic responses during visual stimulation

Stephen D. Mayhew[a], Bradley J. Macintosh[a], Sharon G. Dirckx[a],
Gian Domenico Iannetti[b], Richard G. Wise[c],*

[a]Department of Clinical Neurology, Centre for Functional Magnetic Resonance Imaging of the Brain (FMRIB),
University of Oxford, John Radcliffe Hospital, OX3 9DU Oxford, UK
[b]Department of Neuroscience, Physiology and Pharmacology, University College London, WC1E 6BT London, UK
[c]Cardiff University Brain Research Imaging Centre (CUBRIC), School of Psychology, Cardiff University, Park Place, CF10 3AT Cardiff, UK

Abstract

We investigate the relationship between the temporal variation in the magnitude of occipital visual evoked potentials (VEPs) and of haemodynamic measures of brain activity obtained using both blood oxygenation level dependent (BOLD) and perfusion sensitive (ASL) functional magnetic resonance imaging (fMRI). Volunteers underwent a continuous BOLD fMRI scan and/or a continuous perfusion-sensitive (gradient and spin echo readout) ASL scan, during which 30 second blocks of contrast reversing visual stimuli (at 4 Hz) were interleaved with 30 second blocks of rest (visual fixation). Electroencephalography (EEG) and fMRI were simultaneously recorded and following EEG artefact cleaning, VEPs were averaged across the whole stimulation block (120 reversals, VEP_{120}) and at a finer timescale (15 reversals, VEP_{15}). Both BOLD and ASL time-series were linearly modelled to establish: (1) the mean response to visual stimulation, (2) transient responses at the start and end of each stimulation block, (3) the linear decrease between blocks, (4) the nonlinear between-block variation (covariation with VEP_{120}), (5) the linear decrease within block and (6) the nonlinear variation within block (covariation with VEP_{15}).

VEPs demonstrated a significant linear time-dependent reduction in amplitude, both within and between blocks of stimulation. Consistent with the VEPs finding, both BOLD and perfusion measures showed significant linear time-dependent reductions in response amplitude between blocks. In addition, there were significant linear time-dependent within-block reductions in BOLD response as well as between-block variations positively correlating with VEP_{120} (medial occipital and frontal) and within-block variations positively correlating with VEP_{15} (occipital and thalamus).

Both electrophysiological and haemodynamic (BOLD and ASL) measures of visual activity showed steady habituation through the experiment. Beyond this, the VEP measures were predictive of shorter timescale (3-30 second) localised variations in BOLD response engaging both occipital cortex and other regions such as anterior cingulate and parietal regions, implicating attentional processes in the modulation of the VEP signal.

1. Introduction

Functional magnetic resonance imaging techniques rely on a coupling between changes in neuronal activity and the subsequent haemodynamic response manifested as a blood oxygenation level dependent (BOLD) or perfusion fMRI signal change. The characteristics of that coupling, yielding a change in magnetic resonance (MR) signal on the millimetre spatial scale, depend on the precise aspect of neuronal activity under consideration, such as post-synaptic or spiking in a particular population of neurons [1]; the neurotransmitter (or pharmacological) environment; the spatial extent of electrophysiological activity and the physical properties and physiological state [2] of the cerebral vessels.

Mechanistic studies into the electrophysiology and chemical signalling of neurovascular coupling can be performed invasively in animals [3,4]. Using simultaneous EEG-fMRI in humans, we can take a *brain systems-level*

* Corresponding author. Tel.: +44 2920 870358; fax: +44 2920 870339.
E-mail address: wiserg@cardiff.ac.uk (R.G. Wise).

approach to examining the empirical neurovascular coupling. We describe this as *empirical* coupling because of the spatial and mechanistic distance between activity at the neuronal level and scalp potentials, and the local vascular response and the voxel-scale BOLD/ASL (arterial spin labelling) perfusion signal.

Using fMRI to investigate neurovascular coupling is complicated by the nature of T2*-weighted or BOLD image contrast. BOLD-fMRI relies on changes in local concentrations of deoxyhaemoglobin to localise neuronal activity [5]. In comparison, ASL-fMRI provides a more quantitative measurement of the perfusion of arterial blood into active neuronal tissue and offers potentially improved representation of neural activity compared to BOLD. It has been shown that fMRI measurements of cerebral blood flow (CBF) can be targeted to tissue and capillaries thus avoiding the contributions from large draining veins that can potentially limit the spatial resolution of the BOLD fMRI technique [6].

One of the experimental situations in which it is necessary to record EEG and fMRI simultaneously to investigate the empirical neurovascular coupling is when the brain activity under investigation is unpredictable. In simultaneously acquired data, the EEG is used as a predictor of the haemodynamic activity. For example, in clinical studies of epilepsy, EEG is used to model ictal or interictal discharges in the fMRI time-series [7]. In healthy volunteers, the EEG provides information about the timing and nature of spontaneous brain rhythms for comparison with fMRI during wakefulness [8] and sleep [9]. Simultaneous EEG-fMRI can also be used to investigate time-dependent effects on task-related activity with variable degrees of predictability including drug influences [10], learning, habituation, adaptation [11] and fluctuations in attention or competing cognitive processes.

Visual evoked potentials (VEPs) have been previously recorded simultaneously with fMRI [12–14]. The habituation of VEP amplitude to repetitive stimulation has been reported in previous electrophysiological studies [15,16]. The habituation of both BOLD and VEP amplitudes over a ten minute simultaneous recording duration has been demonstrated [17]. Further studies showed significant decreases in the amplitude of VEP peaks along with the amplitude of the near infrared spectroscopy and fMRI signals in response to 60 and 120s periods of constant visual stimulation [18,19].

Some of the more volatile modulating factors have been successfully investigated by relating trial-to-trial responses of EEG and fMRI [20], in particular using the auditory oddball P300 [21,22] and the error-related negativity [23]. Trial-to-trial co-variation between EEG and fMRI has also been demonstrated in simple auditory stimuli implicating fluctuations in attention through the involvement of the anterior cingulate cortex [24]. In addition to the cognitive processes inducing a common modulation of evoked EEG and fMRI responses, lower level random variations in neuronal firing rates may also contribute [25]. We expect that the different contributions to covariability in EEG and fMRI responses, evoked by visual stimuli, would evolve over different timescales and have their origins, potentially, in different brain regions.

In the present study, we use the amplitude of VEPs as a predictor of haemodynamic activity. We investigate the covariation over time of occipital VEPs and haemodynamic measures of brain activity including both BOLD and perfusion sensitive ASL signal. We hypothesize that the temporal variation in electrophysiological responses over occipital cortex will predict a certain degree of variability in the fMRI response in visual cortex and potential modulating networks. Further, we anticipate that different timescales of VEP variation, from fluctuations of evoked responses over a few seconds to habituation over several minutes, will predict different spatial patterns of covarying fMRI responses, implicating different functional networks in VEP modulation. We investigate both BOLD and CBF fMRI signals to identify the degree to which electrophysiological variation is represented in cerebral perfusion as well as the BOLD response.

2. Methods

The data presented in this study were acquired in two scanning sessions on separate days. Two experiments of simultaneous EEG recordings were performed during fMRI at 3 T using: (1) BOLD contrast, (2) perfusion contrast employing pulsed ASL with gradient and spin echo readout (GRASE-ASL) measurements respectively. Twelve healthy volunteers participated in each experiment: combined cohorts, aged 25-40, 3 females. All subjects gave their informed consent and the procedure was approved by the local ethics committee. Seven subjects took part in both experiments.

2.1. Data acquisition

2.1.1. Visual stimulation

During both BOLD-EEG and ASL-EEG sessions, subjects passively viewed visual stimuli projected onto an acrylic screen via prism glasses. A black and white square checkerboard with a red central fixation cross was presented in a block design of 30-s stimulation followed by 30-s rest. The checkerboard pattern was reversed at a frequency of 4 Hz. The rest condition was a grey screen with the same fixation cross, to which subjects were instructed to attend at all times.

Pattern-reversal VEPs are characterised by a sequence of three major negative-positive-negative peaks spanning approximately 70–180 ms post-stimulus [26]. Here, we adopt the following terminology: N75 at 70–90 ms, P100 at 80–120 ms and N140 at 120–180ms. 4 Hz was chosen as our stimulation frequency in order to maintain a strong evoked BOLD signal and a high number of distinct VEPs, avoiding the overlap of consecutive VEPs that occurs when recording steady-state VEPs.

2.1.2. Experiment 1: BOLD fMRI recording

BOLD fMRI was performed continuously on a Varian INOVA 3T MRI system (Oxford Magnet Technology) with a four-channel, head-only receiver coil. A whole-brain gradient echo, echo-planar imaging sequence was used for the functional scans [TE=30 ms, 43 contiguous 3-mm-thick axial slices (voxel dimensions $3\times3\times3mm^3$), image matrix 64×64] with a repetition time (TR) of 3 s. In each BOLD session 184 volumes were acquired, corresponding to a total scan time of 9 minutes 12 s. During this time, eight blocks of visual stimulation (a total of 960 individual trials) were acquired. A T1-weighted, high-resolution structural image (70 contiguous 3-mm-thick axial slices, in plane field of view 256×192 mm, matrix 256×192) was also collected for anatomical overlay of brain activation and image registration to the Montreal Neurological Institute standard.

2.1.3. Experiment 2: ASL recording

ASL fMRI scanning was performed using a Siemens Trio 3T MRI system. A 12-channel, head-only receiver coil was used. Whole-brain GRASE-ASL perfusion weighted images were collected using a single-shot acquisition at a single inversion time (TI=1200 ms) [27]. ASL images were acquired with the following parameters: TR/TE/TI=3000/39.9/1200 ms, image matrix 64×64×20. Voxel dimensions were 3.125×3.125×5 mm. 180 tag-control image pairs were acquired, corresponding to a total experimental time of 18 min. During this time 16 blocks of visual stimulation (a total of 1920 single-trial VEPs) were acquired. The ASL session was made twice as long as the BOLD session due to the lower SNR of the ASL technique. Low-resolution (3.125×3.125×5 mm) T1-weighted anatomical images were acquired with the same orientation as the GRASE-ASL to facilitate the registration.

2.1.4. EEG recording

During both BOLD and ASL sessions, EEG was recorded from 30 conventional plastic coated Ag/AgCl electrodes according to the 10-20 system. To allow optimal removal of MRI gradient artifacts, a trigger signal was generated from the scanner simultaneously with the RF excitation pulse of every fMRI volume and recorded on the EEG system. Total electrode impedance was kept below 15kΩ (including 10kΩ safety resistors). To monitor ocular movements, eye-blinks and discard contaminated trials, electro-oculographic signals were recorded from bipolar electrodes over the mid-lower eyelid and lateral to the corner of the orbit. To remove the ballistocardiographic pulse artifact, the electrocardiogram (ECG) was also recorded using two chest electrodes. Using the nose as a common reference, EEG data was digitised with an MR-compatible, 22-bit, 32-channel amplifier (SD-MRI, Micromed, Italy) with the following technical characteristics: bandwidth 0.15–600 Hz, sampling rate 2048 Hz, input dynamic range (±26.5 μV, 53 μV peak-to-peak).

2.2. Data analysis

2.2.1. EEG pre-processing

All EEG analysis was conducted using EEGLAB (www.sccn.ucsd.edu/eeglab), an open source toolbox running under the MATLAB environment [28]. Imaging and pulse artifacts present in the EEG data collected during the fMRI session were removed using the FASTR and OBS algorithms [29]. Continuous EEG data were down-sampled to 512 Hz and band-pass filtered from 0.5–45 Hz. Single trials containing the visual stimuli were extracted using a window analysis time of 0.35s (−100 ms pre-stimulus to 250 ms post stimulus) and re-referenced to channel Fz. For each trial, a baseline correction was performed using the pre-stimulus data. Trials contaminated by artifacts due to gross movements were removed following manual inspection. ICA was performed on the single-trial data using the infomax algorithm and components representing eye-blink and movement artifacts were removed from the data [30]. In all data sets, these ICs were identified from scalp maps of electric-field distribution with an obvious frontal weighting and also from bidimensional plots of trial amplitude over time which showed a distinctive pattern of transient deviations with large amplitude occurring at unpredictable latency relative to the stimulus. Furthermore, components that significantly correlated with the recorded ECG signal were rejected as residual BCG artifacts, in accordance with recently published processing strategies [31]. These processing strategies have been recently shown to remove noise artifacts but preserve quality of the stimulus evoked response [24].

2.2.2. VEP amplitude measurements from evoked potential waveforms

Single-trial epochs possess a low signal-to-noise ratio (SNR) that makes it difficult to obtain accurate measurements of the amplitude of VEP components. Therefore, to improve SNR for each individual subject, VEPs (channel O1-ref) were averaged across 15 successive trials to create a "few-trial average", referred to henceforth as VEP_{15}. Thus, every block of visual stimulation was divided into eight periods of 3.75 s, and a VEP_{15} calculated for each. The average VEP was also calculated for each separate block of stimulation using 120 trials (referred to as VEP_{120}).

Both the N75-P100 and the P100-N140 amplitude of each VEP_{15} and VEP_{120} were measured separately for each subject using a multiple-linear regression method [32]. The grand-mean waveform (VEP_{GM}) defined the basis set used to analyse the amplitude of each VEP_{15}, and VEP_{120}. These two different temporal scales of VEP analysis enabled characterisation of the relationship between EEG and fMRI measurements of visual evoked responses. To investigate EEG-fMRI correlations we focus on the most prominent components and therefore all further data analysis in this study uses only the amplitude of the P100-N140 VEP

peaks. Both VEP_{15} and VEP_{120} P100-N140 amplitude measures were included in the fMRI GLM analysis described further below.

2.2.3. BOLD pre-statistical processing

For both BOLD and ASL data, image analysis was performed for each subject using the FMRIB Software Library (FSL) version 4.1 (www.fmrib.ox.ac.uk/fsl). Prior to statistical analysis of BOLD data, the following processing was applied to each subject's time series of fMRI volumes: brain extraction using BET, motion correction using MCFLIRT [33], spatial smoothing using a Gaussian kernel of full width at half maximum 5 mm, subtraction of the mean of each voxel time course from that time course and nonlinear high pass temporal filtering (Gaussian-weighted least squares straight line fitting, with high-pass filter cut-off of 60s). Single-subject time-series statistical analysis was carried out using FILM with local autocorrelation correction. Individual BOLD data were registered to high resolution structural scans and then to standard Montreal Neurological Institute (MNI) template images for group analysis, using FLIRT [34].

2.2.4. ASL pre-statistical processing

For each subject, a sinc-interpolated differencing was used to calculate the GRASE-ASL "tag-control" subtraction [35]. ASL data were spatially normalized and all non-brain areas were removed by masking the data with the subject's low-resolution GRASE-space structural scan. Motion correction was performed using MCFLIRT along with spatial smoothing using a Gaussian kernel of full width at half maximum 8mm, and non linear high pass temporal filtering (Gaussian-weighted least-squares straight line fitting, with high-pass filter cut-off of 60 s).

2.2.5. The BOLD- and ASL-fMRI VEP-informed time-series models

After pre-processing, both BOLD and GRASE-ASL data sets were analysed using the same general linear modeling (GLM) procedure to investigate: (1) whether there are any within- or between-block decreases in the amplitude of the BOLD and CBF responses; (2) whether the BOLD and CBF response amplitudes were correlated with either VEP_{120} or VEP_{15} amplitude measures derived from the EEG.

At the single subject level, a voxel-based analysis of both BOLD and ASL data was performed using a GLM approach with local autocorrelation correction [36] and seven regressors of interest (convolved with a canonical single gamma HRF to model the mean haemodynamic response). See Fig. 1 for an example of a design matrix for an individual BOLD session:

 i. The main checkerboard reversal stimulus (box-car)
 ii. A decreasing linear trend (habituation) within each 30s stimulation block (mean=0 within each block) — *within-block habituation*
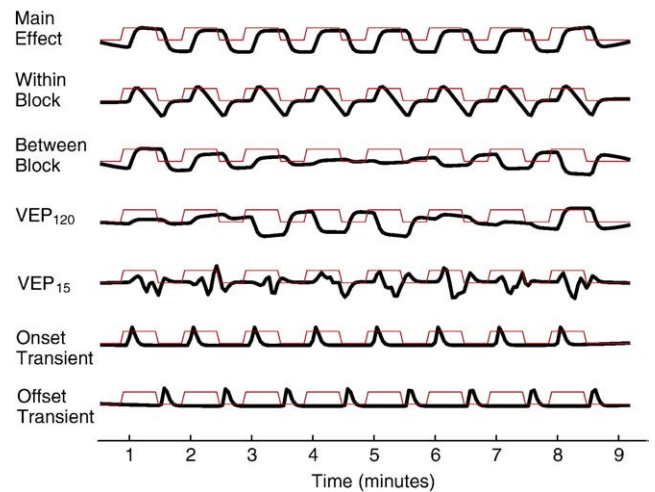

Fig. 1. Example individual design matrix from a BOLD fMRI session (eight blocks of 30-s visual stimulation). Each row represents one of the seven regressors of interest that were used to model the haemodynamic response. All regressors shown here have been convolved with a canonical single gamma HRF. Further, the same temporal filtering is applied to the displayed GLM model as is applied to the fMRI data itself. (i) The main checkerboard reversal stimulus (box-car). (ii) A decreasing linear trend (habituation) within each 30-s stimulation block (mean=0 within each block) — *within-block habituation*. (iii) A decreasing linear trend (habituation) from block to block across the whole experimental session (mean=0 across blocks) — *between-block habituation*; (iv) Block amplitude given by VEP_{120} (mean=0 across blocks and linear trend between blocks removed to orthogonalise with respect to (iii) — *between-block VEP_{120}-related variation* over and above linear decrease. (v) Within block variation of amplitude given by VEP_{15} amplitude (mean=0 within each block and linear trend within blocks removed to orthogonalise with respect to (ii) — *within-block VEP_{15}-related variation* over and above linear decrease. (vi) Transient response at the onset of each stimulation block [37]. (vii) Transient response at the offset of each stimulation block.

 iii. A decreasing linear trend (habituation) from block to block across the whole experimental session (mean=0 across blocks) — *between-block habituation*
 iv. Block amplitude given by simultaneously recorded VEP_{120} (mean=0 across blocks and linear trend between blocks removed to orthogonalise with respect to iii) — *between-block VEP_{120}-related variation* over and above linear decrease
 v. Within block variation of amplitude given by simultaneously recorded VEP_{15} amplitude (mean=0 within each block and linear trend within blocks removed to orthogonalise with respect to ii) — *within-block VEP_{15}-related variation* over and above linear decrease
 vi. Transient response at the onset of each stimulation block [37]
 vii. Transient response at the offset of each stimulation block

Both positive and negative contrasts were set on each regressor to investigate the possibility of increases and decreases in activity both during a stimulation block and

across the experimental session. An additional contrast was set up to assess the significance of both transient responses combined. For both BOLD and CBF datasets, Z-statistic maps of the group (second-level) response to the mean stimulus effect and all regressors representing inter- and within- block trends as well as VEP measures were calculated using a mixed-effects analysis (Z-threshold 2.3, P<.05 cluster corrected) [38].

2.2.6. fMRI region of interest analysis

Five functional regions of interest (ROI) were generated from the brain regions activated by the mean effect of the visual stimulus (orthogonal to the between and within-block variations examined). The thresholded and cluster corrected, mixed effects group maps of the average BOLD and CBF response were considered as one ROI. This was further masked with anatomical masks to create ROIs of: primary visual cortex, inferior lateral occipital cortex, superior lateral occipital cortex and the lateral geniculate nucleus (LGN). Anatomical masks were obtained from the FSL software library (Harvard-Oxford cortical structural atlas). The mean percentage signal change in each ROI associated with the VEP measures was evaluated. The percent signal change was calculated by scaling the contrast of parameter estimate values by one hundred times (100*) the peak-to-peak height of the regressor and then by dividing by the mean over time of the preprocessed time-series data. These are then averaged across all voxels in the ROI.

The signal change for BOLD or CBF was normalized per subject by the relevant magnitude of variability in VEP amplitude (%/μV for BOLD and arbitrary units/μV for CBF). For each subject, the main effect was normalized by the average P100-N140 amplitude, the between-block and within-block habituating trends were normalized by the respective mean decrease in either VEP_{120} or VEP_{15} amplitude. The effects investigating fMRI correlations with VEP_{120} and VEP_{15} were normalized by the mean variability in those VEP measurements, across and within blocks respectively. For each ROI, a paired t test was used to assess whether the mean signal change across the group was statistically different from zero. For a given regressor, a percent signal change across subjects that is significantly different from zero indicates a significant regression between that variable and the fMRI time-series in the voxels of that ROI. This can also be thought of as meaning that the regressor time course and the BOLD time series are significantly correlated in that ROI.

3. Results

3.1. Visual-evoked potentials

3.1.1. Average VEP response

The *few-trial* averaging produced clear and reproducible time-locked VEP_{15} during both BOLD and ASL fMRI

imaging in all subjects. Fig. 2 shows the grand mean VEP_{GM} waveform and scalp maps obtained during both BOLD (red) and ASL acquisition sessions (blue). The earliest identifiable response was the negative N75 component (~75 ms) followed by the positive P100 component (~95 ms) and then the negative N140 (~140 ms). Displayed below the mean waveforms are the respective group mean event related potential (ERP) images which illustrate consistent generation of the VEP response across trials in both the BOLD and ASL sessions. To allow a comparison with the BOLD session, only the first eight blocks of the ASL session were used to make the ERP image. The scalp maps of the ERP display a strong response localised over occipital areas.

3.1.2. Habituation of the P100-N140 VEP amplitude

We measured two time-dependent decreases in the amplitude of the P100-N140 VEP. Firstly, a statistically significant habituation of mean P100-N140 VEP_{15} amplitude *within* 30 s stimulation blocks was observed in both BOLD and ASL sessions, Fig. 2 (linear regression: BOLD R=0.84; P<.01; ASL: R=0.88; P<.01). Furthermore, a statistically significant decrease in the mean P100-N140 VEP_{120} amplitude *between* stimulation blocks was found throughout the course of both the BOLD and ASL experimental sessions. The mean P100-N140 VEP_{120} amplitude for each stimulation block is plotted in Fig. 2 for BOLD (red) and ASL (blue) sessions. During both BOLD and ASL sessions, a significant linear regression was observed between VEP_{120} amplitude and stimulation block number (BOLD: R=0.88; P<.01; ASL: R=0.81; P<.01). No significant decrease in the N75-P100 VEP_{15} amplitude within stimulation blocks was observed (P>.3, data not shown).

3.2. BOLD and CBF fMRI responses to visual stimulation

3.2.1. Average BOLD and CBF responses

Mixed-effects group maps of the average BOLD (red) and CBF (blue) response to the visual block stimulus are displayed in Fig. 3 (main effect). BOLD and CBF activation was observed in primary visual cortex, superior lateral occipital cortex and the LGN. Some differences in the spatial pattern of activation measured by the two techniques were observed. For example, strong BOLD responses were found in bilateral inferior lateral occipital cortex, whereas CBF responses were weak in those areas. In contrast, strong CBF responses were observed in the cuneous and precuneous cortices, but the BOLD response was absent in comparison (discussed further below).

3.2.2. Temporal variation in BOLD and CBF responses

GLM analysis was used to investigate the fMRI response over different time scales and its correlation with measures of N100-P140 VEP amplitude. Significant transient BOLD responses to the onset and offset of block visual stimulation were observed in primary visual cortex, superior lateral
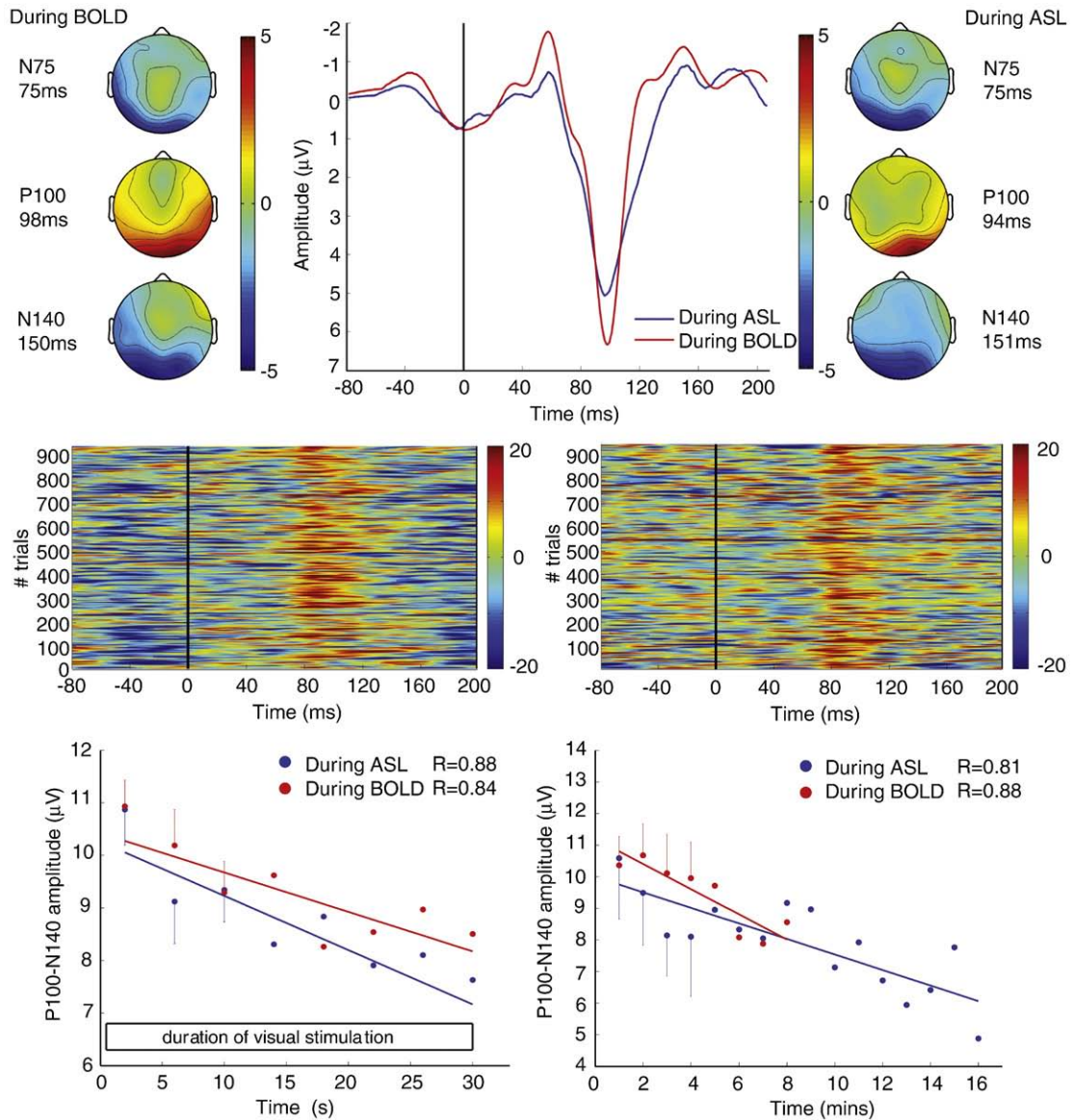
Fig. 2. Group mean VEPs recorded from O1-ref during BOLD and ASL fMRI. (Top) Group-mean waveforms (VEP$_{GM}$) recorded during BOLD (red) and ASL (blue) sessions. Also shown are scalp maps for N75, P100 and N140 components during BOLD (left) and ASL (right) sessions. Middle panel: group ERP images displaying consistency of the single-trial VEP response for the 8 blocks of BOLD session (left) and first 8 blocks of ASL session (right). Lower panel (left): Group mean P100-N140 VEP$_{15}$ amplitudes recorded during ASL (blue) and BOLD (red) stimulation block (left). A significant linear regression was observed between VEP P100-N140 amplitude and stimulation block time (BOLD: R=0.84; P<.01; ASL: R=0.88; P<.01). Gradient of best linear fit, representing rate of habituation, BOLD: −0.32 µV/s; ASL: −0.37 µV/s. Error bars shown for first three mean VEP$_{15}$, standard error in the mean across subjects (S.E.M.). Lower right (right): Group mean P100-N140 VEP$_{120}$ amplitude for each stimulation block recorded during ASL (blue) and BOLD (red) sessions. A statistically significant linear correlation was found for both ASL (R=0.81; P<.01) and BOLD (R=0.88; P<.01). Gradient of best linear-fit, representing rate of habituation, BOLD: −0.36 µV/s; ASL: −0.24 µV/s. Error bars are shown for the first four mean VEP$_{120}$ (S.E.M.) across subjects. (For interpretation of the reference to color in this figure legend, the reader is referred to the web version of this article.)

occipital cortex, the LGN, cingulate cortex, bilateral premotor cortex, supplementary motor cortex and supramarginal gyrus, and right middle frontal gyrus (MFG) (Fig. 3, column 2). In comparison, significant transient CBF responses were observed in primary visual cortex, posterior cingulate and superior lateral occipital cortex (Fig. 3, column 8).

A widespread decrease in the amplitude of BOLD and CBF responses (linear) *between blocks* was observed throughout the duration of the experiment in primary visual areas, but more prominently in lateral occipital cortices as well as the LGN, anterior cingulate cortex (ACC), right inferior frontal cortex, bilateral insula cortex and supramarginal gyrus (Fig. 3, columns 3 and 9). In the ROI analysis the regression of BOLD responses against the between-block linear decreasing trend was found to be statistically different from zero in primary visual areas, lateral occipital cortex and the LGN (P<.05, paired t test). The
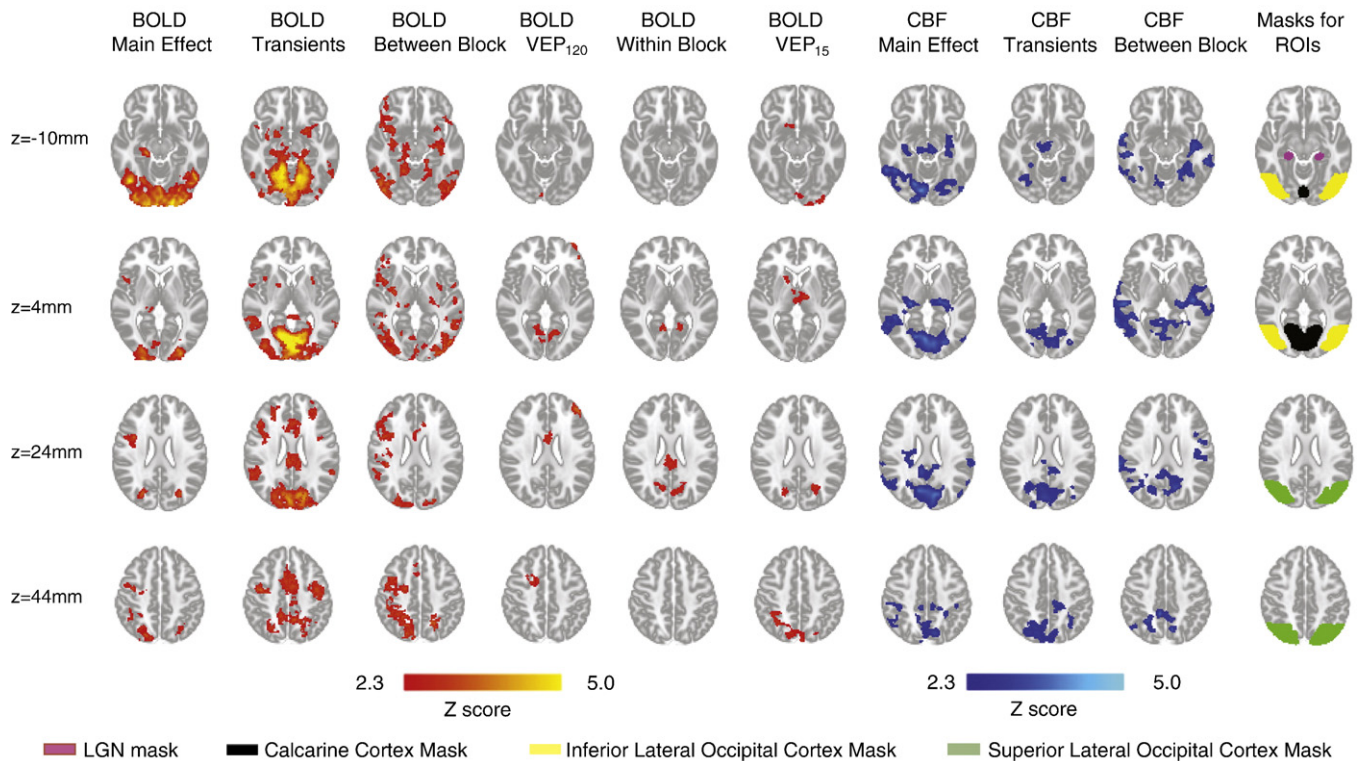
Fig. 3. Mixed effects (cluster-corrected *P*<0.05) group visual-evoked BOLD response (red) and perfusion response (blue) shown superimposed upon the standard MNI brain at four representative axial slices (Talairach coordinates $z=-10$, 4, 24 and 44 mm). For BOLD, each column displays the brain regions where a significant correlation was observed with a separate regressor representing (1) main effect of block stimulation, (2) transient response at onset and offset of block stimulation, (3) linear between-block decrease in response, (4) P100-N140 amplitude of VEP_{120}, (5) linear within-block decrease in response, (6) P100-N140 amplitude of VEP_{15}. Significant CBF results are shown for (1) main effect of block stimulation, (2) transient response at onset and offset of block stimulation, (3) linear between-block decrease in response. No significant results were found in the CBF conditions that are not displayed. The final column illustrates the spatial locations of the anatomical masks used to define ROIs from the main effect of visual stimulation, for both BOLD and CBF responses. LGN, purple; Calcarine cortex, black; inferior lateral occipital cortex, yellow; superior lateral occipital cortex, green. (For interpretation of the reference to color in this figure legend, the reader is referred to the web version of this article.)

CBF response also significantly decreased between stimulation blocks in primary visual cortex and superior lateral occipital cortex (Table 1). No significant BOLD or CBF regression in primary visual cortex was observed in the voxel-wise analysis of the linear decreasing trend *within stimulation* block. However, a significant regression was observed in cuneous cortex and posterior cingulate cortex (PCC) for BOLD (mixed effects *z*>2.3; cluster *P*=.05) that correlated with a decreasing trend within-blocks (Fig. 3, column 5). In the ROI analysis, a significant regression between the decreasing within-block linear trend and the CBF response was observed in primary visual areas (*P*<.05) (Table 1).

BOLD activity was observed to correlate with the P100-N140 amplitude of the VEP_{120}, between-block over and above a linear decreasing trend, in primary visual cortex, cuneous cortex, ACC and bilateral MFG (Fig. 3, column 4). In the ROI analysis, significant correlations were also found between the amplitude of the VEP_{120} and the percent BOLD signal change evoked by a block of visual stimulation (Table 1) in the whole functional ROI and the calcarine cortex (*P*<.05). The CBF signal change was mostly significantly correlated with VEP_{120} amplitude in the whole functional ROI and intracalcarine cortex (*P*<.01). Significant correlations were also observed in V1 and in bilateral lateral occipital cortex (*P*<.05). Furthermore, voxel-wise correlations, within-block over and above a linear decreasing trend, between the amplitude of the BOLD signal and the VEP_{15} P100-N140 were observed in superior lateral occipital cortex and thalamus (Fig. 3, column 6).

4. Discussion

In this study we compare the temporal variation of the EEG and BOLD / ASL-fMRI response amplitudes both within (on a timescale of seconds) and between (on a timescale of a few minutes) repeated blocks of visual stimulation. The EEG and fMRI responses are well correlated between blocks, thus suggesting that the between-block habituation of the BOLD and CBF responses is of neuronal origin. The within block temporal variation of EEG and fMRI responses correlated in a few regions, different from those in which the between-blocks correlation was observed.

Table 1
Results of functional ROI analysis and anatomically constrained functional ROI analysis of BOLD and CBF responses

	Whole functional region	Calcarine Cortex	Inferior lateral occipital	Superior lateral occipital	LGN
BOLD	%/μV	%/μV	%/μV	%/μV	%/μV
Main effect	0.16±0.06 *	0.23±0.08 *	0.16±0.05 *	0.09±0.03 *	0.06±0.02 *
Between block	0.17±0.08 *	0.18±0.09 *	0.21±0.1 *	0.16±0.08 *	0.13±0.06 *
Within block	0.05±0.12	0.05±0.11	0.07±0.14	0.02±0.14	0.03±0.16
VEP$_{120}$	0.09±0.04 *	0.12±0.05 *	0.07±0.05	0.03±0.04	0.07±0.05
VEP$_{15}$	0.03±0.05	0.02±0.03	0.01±0.06	0.01±0.02	0.01±0.02
ASL	arb. unit/μV	arb. unit/μV	arb. unit/μV	arb. unit/μV	arb. unit/μV
Main effect	0.29±0.12 *	0.17±0.06 *	0.22±0.1 *	0.1±0.04 *	0.07±0.04 *
Between block	0.19±0.1 *	0.17±0.09 *	0.06±0.12	0.18±0.08 *	0.07±0.14
Within block	0.25±0.21	0.27±0.1 *	0.12±0.11	0.2±0.17	0.09±0.16
VEP$_{120}$	0.04±0.06	0.04±0.03	0.03±0.08	0.05±0.03	0.02±0.02
VEP$_{15}$	0.03±0.04	0.02±0.03	0.06±0.07	0.03±0.03	0.02±0.04

In each ROI, the signal change is calculated from the regression of each of five effects of interest: main effect of stimulation, between-block linear decrease, within-block linear decrease, VEP$_{120}$ amplitude variability, VEP$_{15}$ amplitude variability. Each effect was normalized per subject by the appropriate variability in P100-N140 VEP amplitude (%/μV).

* Denotes that the regression of that effect is statistically different from zero ($P<.05$).

4.1. Short- and long-term habituation of the visual evoked response

In this study we observed a significant habituation of VEP P100-N140 amplitude both within and between 30-s stimulation blocks (Fig. 2). Modeling a linearly decreasing trend throughout the experiment revealed a significant regression for both BOLD and CBF, though the BOLD response was observed to habituate in a more extensive network of areas than the CBF response. Between-block decreases in both BOLD and CBF were observed in primary visual cortex. However, the most significant BOLD and CBF decreases between blocks were observed in inferior lateral occipital cortices. This result suggests that secondary visual areas responsible for motion, texture and object processing adapt to the repeated task demands more than primary visual areas over the experiment duration. The statistical maps were supported by the results of an ROI analysis which showed a significant regression with a decreasing linear trend between stimulation blocks in primary visual areas as well as in extrastriate regions and LGN for both BOLD and CBF. The ROI analysis estimated the magnitude of the linear habituation between blocks as approximately a 0.2% change in BOLD signal per μV decrease in VEP amplitude (Table 1).

Previous fMRI studies of sustained visual stimulation report contrasting findings of: elevated BOLD responses throughout 10 min of constant stimulation [39]; an approximate 50% reduction in signal for constant stimulation periods between 200 and 500 s [40,41], and no significant signal decreases over 1200-s stimulation [42,43]. However, none of these studies directly measured the neuronal activity underlying the BOLD and CBF signals. The habituation of both BOLD and VEP amplitudes over a 10-min simultaneous recording duration has been reported [17]. Within stimulus blocks of 30s duration we observed habituation of the P100-N140 amplitude. The associated decrease in the BOLD response averaged together over all of the function-ally-defined visual regions did not reach statistical significance. In the voxel-wise analysis, a small region of significant regression between the within-block decreasing linear trend and the BOLD response at the extreme anterior part of calcarine cortex was observed. The ROI analysis showed no significant regression between the BOLD response and the within-block trend for any of the regions tested. However, a significant regression of within-block decreases in CBF response was observed in calcarine cortex (Table 1). These results suggest that the CBF response maybe more tightly coupled to underlying habituating neuronal activity than the BOLD response.

4.2. Sources of the VEP and relationship to changes in fMRI response

We observed no significant change in amplitude of the N75-P100 amplitude within stimulation blocks. Intracortical electrode studies in monkeys identified the origin of the three primary VEP components in primary visual cortex [44]. Recent combinations of EEG source localization with the cortical areas of positive fMRI response have placed the generators of the N75 component within the calcarine fissure of the primary visual cortex [26,45,46]. The P100 is also believed to originate from striate cortex [26,46] although extrastriate generators have been proposed [47]. The exact origin of the N140 peak remains disputed. Considering these localization studies, a possible explanation for our lack of large habituation effects in primary visual cortex with fMRI measurements could be that the neural activity measured by fMRI is maintained, as represented to some extent by the activities underlying earliest N75 peak of the VEP. Recently, the P100 has been shown to co-localise with negative BOLD responses in anterior calcarine cortex [46]. In this study, we did not observe any significant negative fMRI responses in visual cortex; therefore, we were unable to investigate this further.

4.3. Attentional modulation of visual responses

It has been widely demonstrated that attention modulates the magnitude of the neuronal response to a visual stimulus in V1, V2, V3, V4, MT, the LGN and posterior parietal areas [48]. Single-cell recordings in monkeys [49] and fMRI recordings [50] in humans have all shown an increase in the magnitude of the neural response in both striate and extra-striate cortex when the stimulus is attended, compared to an unattended condition.

In this study, extrastriate BOLD responses that correlate with decreasing linear trends in VEPs were observed between-block in left MFG and the ACC and within-block in cuneous/parietal-occipital sulcus cortex and PCC, suggesting attentional modulation of the response. Neither the cuneous or PCC has been identified as possible sources of the VEP; therefore, any role these regions have in modulating visual activity is most likely to be an indirect, top-down effect upon more primary visual areas. The parieto-occipital sulcus has a proposed role in modulating attentional demand [51]. A recent magnetoencephalography (MEG) study has shown that the magnitude of oscillatory activity in the calcarine and parieto-occipital (PO) sulci was dependent on the attentional status of the observer [52]. Enhanced activity in contralateral calcarine hemisphere, and ipsilateral PO hemisphere in the alpha band was found in response to the direction of spatial attention. This is in agreement with other studies reporting increased alpha activity over occipital cortex related to the direction of spatial attention [53].

4.4. Correlations between VEP and fMRI amplitudes beyond the linear variation with time

Using a multiple linear regression measurement technique we measured P100-N140 amplitudes from VEP waveforms, averaged over timescales of four (VEP_{15}) and 30 (VEP_{120}) s, and we assessed the correlation of these averages with the BOLD- and ASL-fMRI signals using a GLM analysis. We have observed significant BOLD-VEP correlations both at 4 and 30 s timescales (Fig. 3, Table 1). In the voxel-wise analysis, the amplitude of both VEP_{15} and VEP_{120} were observed to correlate with BOLD signal in primary visual cortex, with VEP_{15} also significantly correlating with BOLD in superior lateral occipital cortex. These correlations reflect common variability in EEG and fMRI measurements over and above the linear time-dependent decreases between and within block. The ROI analysis estimated the magnitude of this correlation to be approximately 0.1% change in BOLD signal per μV variability in VEP amplitude (Table 1).

Beyond the linear trends, no correlations between the amplitude of VEPs and the CBF response were observed in this study. Previously, a significant linear coupling of CBF and VEP amplitude has been reported [54] using Doppler ultrasound measures and variable image contrast. Our result probably reflects the weaker signal-to-noise ratio (SNR) of ASL-fMRI compared to BOLD and the

inherent temporal averaging in ASL-fMRI. Z-scores of mixed effects analysis of the CBF and BOLD mean effect were approximately equivalent (Fig. 3), which can be partly explained by the higher SNR of GRASE compared to other ASL techniques [27] and also by the doubled length of stimulation in the ASL session. The temporal resolution of ASL-fMRI is poorer than that of BOLD because of the necessity to form tag and control images and to allow time for blood to be delivered from the tagging region to the imaging slice. In this study, each tag and control image pair took 6s to acquire, which was double the BOLD TR of 3s.

4.5. BOLD and CBF responses to the main effect of visual stimulation

Several differences in spatial extent of BOLD and CBF responses to the main effect of visual stimulation were observed in extra-striate cortex. BOLD responses were observed in bilateral lateral occipital cortex, bilateral supramarginal gyrus, right precentral gyrus and angular gyrus. In comparison, CBF responses were measured in bilateral lateral occipital cortex, cuneous and precuneous cortex and right supramarginal gyrus (Fig. 3). Some of the differences in spatial extent of these extrastriate activations could be attributed to the smearing of the CBF signal in the z-direction that is inherent in the GRASE ASL acquisition. This effect arises due to the long series of spin-echoes employed to allow single shot 3D acquisition. Consequently, the spatial localisation of the CBF response is sub-optimal because of: (1) the blurring of the signal in the z-direction deriving from the acquisition process and (2) the inhomogeneous signal intensity across the imaging volume in the anterior-posterior direction. Signal intensity across the image plane is influenced by the profile of the B_1 magnetic field, which will affect tagging efficiency across the brain.

4.6. Transient fMRI responses to stimulation onset and offset

In addition to the main effect, we also demonstrate significant transient BOLD and CBF responses to the onset and offset of block stimulation in primary visual cortex (Fig. 3). CBF transient responses are more specifically localized to V1 than BOLD responses which are observed in a large network including the LGN, superior lateral occipital cortex. Responses detected in the cingulate cortex and bilateral premotor cortex can likely be attributed to changes in the attentional state of the subject at the transition between stimulation and rest. Transient BOLD and CBF responses to visual stimulation have been previously reported [37], but to our knowledge, this is the first demonstration of the spatial extent of both BOLD and CBF transients to block visual stimulation. It has been recently debated whether transient BOLD responses have a neuronal [55] or a vascular origin [56].

4.7. Empirical neurovascular coupling between VEPs and fMRI

We report widespread correlation between VEP and both BOLD- and ASL-fMRI signal amplitudes over the ten minute duration of the experiment. However, the less extensive association between EEG and fMRI measurements observed at the within-block timescale could be attributed to the different physiological origins of the EEG and fMRI signals. VEPs provide a limited representation of the total neural activity at any given instant of visual processing and in our study are restricted to the occipital pole. VEPs are a transient change in the ongoing EEG signal, created by the summation of synchronous neural activities in favourably aligned cortical pyramidal cells and are sensitive to conduction through the brain and skull, and the possible cancellation of opposing current sources. In contrast, the BOLD signal integrates time-locked and non time-locked synaptic inputs of the entire neuronal population to a region regardless of the orientation, or the excitatory or inhibitory role of those neurons. Although in this study we report no significant correlations between the amplitudes of the VEP and the CBF response, previous work suggests that the CBF signal may be more localized to the underlying neuronal activity than BOLD measurements [57]. In several studies, ASL measures have been shown to possess decreased inter subject and inter session variability compared to BOLD, a finding interpreted as reflecting a more direct link to neural activity [58–60].

In this study we have used linear regression to investigate the behaviour of EEG and fMRI responses at different time scales. Therefore, we are not sensitive to detect nonlinearities that might exist in the relationship between the two measurements. Recent studies have demonstrated nonlinear relationships between the haemodynamic response and local electrophysiological activity [61–63]. It is suggested that this discrepancy is due to the haemodynamic response at a given location reflecting the integration of electrophysiological activity over a spatial scale larger than the typical dimensions of an fMRI voxel. Therefore, the strongest correlation of BOLD and EEG might be found at a regional scale, as indicated by the significant VEP_{120}-BOLD correlations in calcarine cortex found in our ROI analysis.

The temporal covariation of VEPs and fMRI does not necessarily imply common sources for both signals as there may be, for example, modulators common to both but directly visible to neither technique. We relate that part of the neuronal activity detectable at the scalp to a haemodynamic response which may arise from a different portion of neural tissue. So what value are these measurements? By examining common temporal variance between EEG and fMRI, the EEG measure can tell us about the behaviour of the fMRI network. Conversely the patterns of fMRI-covarying activity indicate potential mechanisms underlying the modulation of the source of the electrophysiological activity. The patterns associated with different timescales of modulation implicate different systems-level mechanisms in modulating the VEPs, such as habituation and fluctuations in attention.

References

[1] Logothetis NK. What we can do and what we cannot do with FMRI. Nature 2008;453(7197):869–78.

[2] Brown GG, Eyler Zorrilla LT, Georgy B, Kindermann SS, Wong EC, Buxton RB. BOLD and perfusion response to finger-thumb apposition after acetazolamide administration: differential relationship to global perfusion. J Cereb Blood Flow Metab 2003;23(7): 829–37.

[3] Logothetis NK, Pauls J, Augath M, Trinath T, Oeltermann A. Neurophysiological investigation of the basis of the FMRI signal. Nature 2001;412(6843):150–7.

[4] Goense JB, Logothetis NK. Neurophysiology of the BOLD FMRI signal in awake monkeys. Curr Biol 2008;18(9):631–40.

[5] Kwong KK, Belliveau JW, Chesler DA, et al. Dynamic magnetic resonance imaging of human brain activity during primary sensory stimulation. Proc Natl Acad Sci USA 1992;89(12):5675–9.

[6] Kim DS, Ronen I, Olman C, Kim SG, Ugurbil K, Toth LJ. Spatial relationship between neuronal activity and BOLD functional MRI. Neuroimage 2004;21(3):876–85.

[7] Gotman J. Epileptic networks studied with EEG-FMRI. Epilepsia 2008;49(Suppl 3):42–51.

[8] Goldman RI, Stern JM, Engel Jr J, Cohen MS. Simultaneous EEG and FMRI of the alpha rhythm. Neuroreport 2002;13(18):2487–92.

[9] Schabus M, Dang-Vu TT, Albouy G, et al. Hemodynamic cerebral correlates of sleep spindles during human non-rapid eye movement sleep. Proc Natl Acad Sci USA 2007;104(32):13164–9.

[10] Iannetti GD, Wise RG. BOLD functional MRI in disease and pharmacological studies: room for improvement? Magn Reson Imaging 2007;25(6):978–88.

[11] Grill-Spector K, Henson R, Martin A. Repetition and the brain: neural models of stimulus-specific effects. Trends Cogn Sci 2006;10(1): 14–23.

[12] Bonmassar G, Anami K, Ives J, Belliveau JW. Visual evoked potential (VEP) measured by simultaneous 64-channel EEG and 3T FMRI. Neuroreport 1999;10(9):1893–7.

[13] Kruggel F, Herrmann CS, Wiggins CJ, von Cramon DY. Hemodynamic and electroencephalographic responses to illusory figures: recording of the evoked potentials during functional MRI. Neuroimage 2001;14(6):1327–36.

[14] Sommer M, Meinhardt J, Volz HP. Combined measurement of event-related potentials (ERPs) and FMRI. Acta Neurobiol Exp (Wars) 2003;63(1):49–53.

[15] Wastell DG, Kleinman D. Potentiation of the habituation of human brain potentials. Biol Psychol 1980;10(1):21–9.

[16] Peachey NS, DeMarco Jr PJ, Ubilluz R, Yee W. Short-term changes in the response characteristics of the human visual evoked potential. Vision Res 1994;34(21):2823–31.

[17] Bianciardi M, Bianchi L, Garreffa G, et al. Single-epoch analysis of interleaved evoked potentials and FMRI responses during steady-state visual stimulation. Clin Neurophysiol 2009;120(4):738–47.

[18] Obrig H, Israel H, Kohl-Bareis M, et al. Habituation of the visually evoked potential and its vascular response: implications for

neurovascular coupling in the healthy adult. Neuroimage 2002;17(1): 1–18.

[19] Janz C, Heinrich SP, Kornmayer J, Bach M, Hennig J. Coupling of neural activity and BOLD FMRI response: new insights by combination of FMRI and VEP experiments in transition from single events to continuous stimulation. Magn Reson Med 2001;46 (3):482–6.

[20] Debener S, Ullsperger M, Siegel M, Engel AK. Towards single-trial analysis in cognitive brain research. Trends Cogn Sci 2007;11(12): 502–3.

[21] Eichele T, Specht K, Moosmann M, et al. Assessing the spatiotemporal evolution of neuronal activation with single-trial event-related potentials and functional MRI. Proc Natl Acad Sci USA 2005;102 (49):17798–803.

[22] Benar CG, Schon D, Grimault S, et al. Single-trial analysis of oddball event-related potentials in simultaneous EEG-FMRI. Hum Brain Mapp 2007;28(7):602–13.

[23] Debener S, Ullsperger M, Siegel M, Fiehler K, von Cramon DY, Engel AK. Trial-by-trial coupling of concurrent electroencephalo-gram and functional magnetic resonance imaging identifies the dynamics of performance monitoring. J Neurosci 2005;25(50): 11730–7.

[24] Mayhew SD, Dirckx SG, Niazy RK, Iannetti GD, Wise RG. EEG signatures of auditory activity correlate with simultaneously recorded FMRI responses in humans. Neuroimage 2009;49(1):849–64.

[25] Faisal AA, Selen LP, Wolpert DM. Noise in the nervous system. Nat Rev Neurosci 2008;9(4):292–303.

[26] Di Russo F, Pitzalis S, Spitoni G, et al. Identification of the neural sources of the pattern-reversal VEP. Neuroimage 2005;24(3):874–86.

[27] Gunther M, Oshio K, Feinberg DA. Single-shot 3D imaging techniques improve arterial spin labeling perfusion measurements. Magn Reson Med 2005;54(2):491–8.

[28] Delorme A, Makeig S. EEGLAB: an open source toolbox for analysis of single-trial EEG dynamics including independent component analysis. J Neurosci Methods 2004;134(1):9–21.

[29] Niazy RK, Beckmann CF, Iannetti GD, Brady JM, Smith SM. Removal of FMRI environment artifacts from EEG data using optimal basis sets. Neuroimage 2005;28(3):720–37.

[30] Jung TP, Makeig S, Westerfield M, Townsend J, Courchesne E, Sejnowski TJ. Removal of eye activity artifacts from visual event-related potentials in normal and clinical subjects. Clin Neurophysiol 2000;111(10):1745–58.

[31] Srivastava G, Crottaz-Herbette S, Lau KM, Glover GH, Menon V. ICA-based procedures for removing ballistocardiogram artifacts from EEG data acquired in the MRI scanner. Neuroimage 2005;24(1): 50–60.

[32] Mayhew SD, Iannetti GD, Woolrich MW, Wise RG. Automated single-trial measurement of amplitude and latency of laser-evoked potentials (LEPs) using multiple linear regression. Clin Neurophysiol 2006;117(6):1331–44.

[33] Jenkinson M, Bannister P, Brady M, Smith S. Improved optimization for the robust and accurate linear registration and motion correction of brain images. Neuroimage 2002;17(2):825–41.

[34] Jenkinson M, Smith S. A global optimisation method for robust affine registration of brain images. Med Image Anal 2001;5(2): 143–56.

[35] Mumford JA, Hernandez-Garcia L, Lee GR, Nichols TE. Estimation efficiency and statistical power in arterial spin labeling FMRI. Neuroimage 2006;33(1):103–14.

[36] Woolrich MW, Ripley BD, Brady M, Smith SM. Temporal autocorrelation in univariate linear modeling of FMRI data. Neuro-image 2001;14(6):1370–86.

[37] Uludag K. Transient and sustained BOLD responses to sustained visual stimulation. Magn Reson Imaging 2008;26(7):863–9.

[38] Woolrich MW, Behrens TE, Beckmann CF, Jenkinson M, Smith SM. Multilevel linear modelling for FMRI group analysis using Bayesian inference. Neuroimage 2004;21(4):1732–47.

[39] Howseman AM, Porter DA, Hutton C, Josephs O, Turner R. Blood oxygenation level dependent signal time courses during prolonged visual stimulation. Magn Reson Imaging 1998;16(1):1–11.

[40] Frahm J, Kruger G, Merboldt KD, Kleinschmidt A. Dynamic uncoupling and recoupling of perfusion and oxidative metabolism during focal brain activation in man. Magn Reson Med 1996;35(2): 143–8.

[41] Hathout GM, Kirlew KA, So GJ, et al. MR imaging signal response to sustained stimulation in human visual cortex. J Magn Reson Imaging 1994;4(4):537–43.

[42] Bandettini PA, Kwong KK, Davis TL, et al. Characterization of cerebral blood oxygenation and flow changes during prolonged brain activation. Hum Brain Mapp 1997;5(2):93–109.

[43] Chen W, Zhu XH, Kato T, Andersen P, Ugurbil K. Spatial and temporal differentiation of FMRI BOLD response in primary visual cortex of human brain during sustained visual simulation. Magn Reson Med 1998;39(4):520–7.

[44] Kraut MA, Arezzo JC, Vaughan Jr HG. Intracortical generators of the flash VEP in monkeys. Electroencephalogr Clin Neurophysiol 1985;62 (4):300–12.

[45] Vanni S, Warnking J, Dojat M, Delon-Martin C, Bullier J, Segebarth C. Sequence of pattern onset responses in the human visual areas: an FMRI constrained VEP source analysis. Neuroimage 2004;21(3): 801–17.

[46] Whittingstall K, Stroink G, Schmidt M. Evaluating the spatial relationship of event-related potential and functional MRI sources in the primary visual cortex. Hum Brain Mapp 2007;28(2):134–42.

[47] Clark VP, Fan S, Hillyard SA. Identification of early visually evoked potential generators by retinotopic and topographic analysis. Hum Brain Mapp 1995;2:170–87.

[48] Somers DC, Dale AM, Seiffert AE, Tootell RB. Functional MRI reveals spatially specific attentional modulation in human primary visual cortex. Proc Natl Acad Sci USA 1999;96(4):1663–8.

[49] Vidyasagar TR. Gating of neuronal responses in macaque primary visual cortex by an attentional spotlight. Neuroreport 1998;9(9): 1947–52.

[50] Tootell RB, Mendola JD, Hadjikhani NK, et al. Functional analysis of V3A and related areas in human visual cortex. J Neurosci 1997;17(18): 7060–78.

[51] Vanni S, Revonsuo A, Hari R. Modulation of the parieto-occipital alpha rhythm during object detection. J Neurosci 1997;17(18):7141–7.

[52] Yamagishi N, Callan DE, Goda N, Anderson SJ, Yoshida Y, Kawato M. Attentional modulation of oscillatory activity in human visual cortex. Neuroimage 2003;20(1):98–113.

[53] Jensen O, Gelfand J, Kounios J, Lisman JE. Oscillations in the alpha band (9-12 Hz) increase with memory load during retention in a short-term memory task. Cereb Cortex 2002;12(8):877–82.

[54] Zaletel M, Strucl M, Rodi Z, Zvan B. The relationship between visually evoked cerebral blood flow velocity responses and visual-evoked potentials. Neuroimage 2004;22(4):1784–9.

[55] Fox MD, Snyder AZ, McAvoy MP, Barch DM, Raichle ME. The BOLD onset transient: identification of novel functional differences in schizophrenia. Neuroimage 2005;25(3):771–82.

[56] Obata T, Liu TT, Miller KL, et al. Discrepancies between BOLD and flow dynamics in primary and supplementary motor areas: application of the balloon model to the interpretation of BOLD transients. Neuroimage 2004;21(1):144–53.

[57] Duong TQ, Kim DS, Ugurbil K, Kim SG. Localized cerebral blood flow response at submillimeter columnar resolution. Proc Natl Acad Sci USA 2001;98(19):10904–9.

[58] Aguirre GK, Detre JA, Zarahn E, Alsop DC. Experimental design and the relative sensitivity of BOLD and perfusion FMRI. Neuroimage 2002;15(3):488–500.

[59] Tjandra T, Brooks JC, Figueiredo P, Wise R, Matthews PM, Tracey I. Quantitative assessment of the reproducibility of functional activation measured with BOLD and MR perfusion imaging: implications for clinical trial design. Neuroimage 2005;27(2):393–401.

[60] Wang J, Aguirre GK, Kimberg DY, Roc AC, Li L, Detre JA. Arterial spin labeling perfusion FMRI with very low task frequency. Magn Reson Med 2003;49(5):796–802.

[61] Devor A, Dunn AK, Andermann ML, Ulbert I, Boas DA, Dale AM. Coupling of total hemoglobin concentration, oxygenation, and neural activity in rat somatosensory cortex. Neuron 2003;39(2): 353–9.

[62] Jones M, Hewson-Stoate N, Martindale J, Redgrave P, Mayhew J. Nonlinear coupling of neural activity and CBF in rodent barrel cortex. Neuroimage 2004;22(2):956–65.

[63] Wan X, Riera J, Iwata K, Takahashi M, Wakabayashi T, Kawashima R. The neural basis of the hemodynamic response nonlinearity in human primary visual cortex: Implications for neurovascular coupling mechanism. Neuroimage 2006;32(2):616–25.